AD-A188 890 NONLINEAR RESONANCE OF TWO-DIMENSIONAL ION LAYERS(U) 1/1
CALIFORNIA UNIV LOS ANGELES CENTER FOR PLASMA PHYSICS
AND FUSION ENGINEERING S A PRASAD ET AL. SEP 87
UNCLASSIFIED PPG-1106 N00014-84-K-0503 F/G 20/3 NL

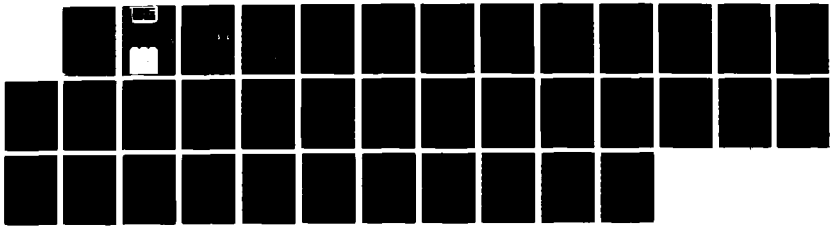

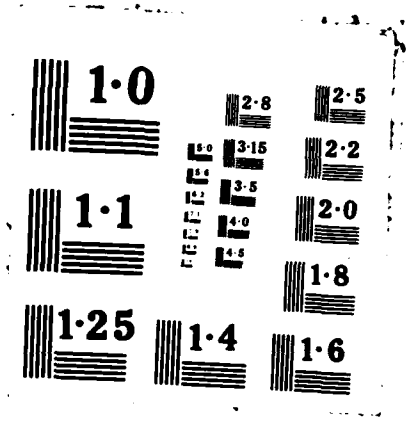
1·0
1·1
1·25
1·4
1·6
1·8
2·0
2·2
2·5
2·8
3·15
3·5
4·0
4·5

UCLA

"Nonlinear Resonance of Two-Dimensional Ion Layers"

S. A. Prasad and G. J. Morales

September, 1987 PPG-1106

Contract N00014-84-K-0583

CENTER FOR
PLASMA PHYSICS
AND
FUSION ENGINEERING

UNIVERSITY OF CALIFORNIA
LOS ANGELES

(2)

"Nonlinear Resonance of Two-Dimensional Ion Layers"

S. A. Prasad and G. J. Morales

September, 1987 PPG-1106

Contract N00014-84-K-0583

Department of Physics

University of California, Los Angeles

Los Angeles, CA 90024

NONLINEAR RESONANCE OF TWO-DIMENSIONAL ION LAYERS

S. A. Prasad and G. J. Morales

Physics Department

University of California at Los Angeles

Los Angeles, CA 90024-1547

A nonlinear theory of wave resonances in a two-dimensional ion layer confined under the surface of liquid helium is presented. The ion layer is modelled as a two-dimensional cold plasma fluid. In addition to the usual nonlinearities present in the continuity equation and the equation of motion, the theory considers a nonlinear dependence of the mass of a plasma particle on its velocity, as suggested by indirect experimental evidence. Secular perturbation theory is used to find the plasma response when the damped, nonlinear system is driven externally. For typical experimental parameters, the mass nonlinearity is found to be the dominant nonlinear effect, giving rise to a backbending of the resonance curve.

over

Pacs: 52.35 MW, 52.25 Wz, 52.35 Fp

I. INTRODUCTION

Helium ions can be trapped just below the surface of superfluid helium.[1,2] These ions form an almost ideal two-dimensional layer held in position by external electrostatic fields. Waves can be excited in the ion layer by an oscillating electric potential applied to the walls of the confining cell. As the amplitude of the applied potential is increased, the waves are observed[1] to display nonlinear features such as hysteresis, indicative of a backbending of the resonance curve. It is the purpose of the present study to provide an analytical description of such phenomena.

The linear properties of waves in these systems can be accurately described[3] by modelling the ions as a cold two-dimensional fluid plasma. Such a model is used in this study to explain the nonlinear behavior. The first source of nonlinearity considered here arises from the nonlinear terms in the continuity equation and the equation of motion (the ponderomotive effect term) which describe the fluid motion in the plane of the ion layer. The second source of nonlinearity considered is a dependence of the mass of the plasma particle on its velocity. A brief discussion of what a plasma particle is in these systems is presented next to motivate this proposed nonlinearity.

Helium is in the liquid state at typical experimental temperatures ($\lesssim$ 0.2 K) and no external pressure. The presence of an He^+ ion in the liquid polarizes the surrounding helium atoms and provides enough local pressure (due to electrostatic attraction) to freeze a sphere of about 25 helium atoms around each ion. Since this object moves in a liquid, its effective mass is further enhanced[4] by half the mass of the displaced fluid. Thus the effective mass of a singly charged plasma particle is expected to be approximately 150 a.u..

A fit of experimental data[1] with linear wave theory yields similar values. However, it has been experimentally observed[1] that the effective mass obtained by the best fit between theory and experiments increases with the temperature of the liquid helium (in addition to depending on the external confining fields and the ion density). For the temperature range in Ref. 1 (0.1 -0.5 K), the dependence is nearly linear. The microscopic reason for this dependence is not yet fully understood. Nevertheless, one can hypothesize that the increase in mass m is associated with the thermal motion of the particle and that an oscillatory motion with a velocity $\underset{\sim}{v}$ (caused, for example, by a wave) is equivalent to an effective temperature $T_{eff} = m|v|^2/2$ (for two-dimensional motion or twice this value for one-dimensional motion). This leads to a dependence $m = m_o[1 + \beta|\underset{\sim}{v}|^2]$ where the coefficients m_o and β depend on the external holding fields and the static ion charge density. The value of β in typical experiments[1] is on the order of 10^{-7} $cm^{-2}s^2$.

The experiments on ion layers have typically employed a cylindrical geometry and efforts are now underway to use a rectangular geometry. In the present work, the simpler Cartesian model is emphasized for clarity of exposition, but the corresponding results for the cylindrical case are also described. Previous work[2] on the nonlinear waves in Cartesian two-dimensional plasmas makes idealized assumptions on the equilibrium density profile and uses boundary conditions (satisfied by the wave potential) which are not well justified; furthermore, only the ponderomotive nonlinearity is considered. The goal of the present work is to present a rigorous treatment,

cont'd
including exact equilibrium profiles and correct boundary conditions, of the nonlinearities present in the continuity equation and the equation of motion as well as the mass nonlinearity.

The paper is organized as follows. The Cartesian geometry of the model and the basic cold plasma fluid equations satisfied by the ion system are described in Sec. II. Secular perturbation theory is used to solve the nonlinear equations. Static equilibrium described by the zeroth order equations is obtained in Sec. III. The first order equations comprise an eigenvalue problem for the wave potential and are discussed in Sec. IV. Solutions to these equations exist only for certain eigenvalues of the frequency. Included in the analysis of the second order equations (Sec. V) are the static ponderomotive potential as well as the plasma response at the second harmonic. Analysis of the third order plasma response at the fundamental frequency is presented in Sec. VI. The homogeneous part of the equation is identical to the first order equation and therefore the existence of a finite solution requires that the inhomogeneous part must be orthogonal to the first order solution. This condition yields the shift in the linear resonance frequency caused by the various nonlinear terms considered. It is found that the dominant contribution in a typical experimental ion layer is the mass nonlinearity which gives rise to a backbending of the resonant curve. The analogous results for cylindrical geometry are presented in Sec. VII. Conclusions are presented in Sec. VIII.

II. GEOMETRY AND BASIC EQUATIONS

The Cartesian model geometry is shown in Fig. 1. A two-dimensional plasma strip, translationally invariant in y (i.e., perpendicular to the plane of the paper) and of width 2a in the x-direction is confined at z = d by equilibrium external potentials ϕ_{t0} , 0 and ϕ_{b0} applied to the top, side and bottom of a confinement cell of width 2L and height h. The ions are held just below the liquid helium surface by the combined effect[3] of the external holding fields and the dielectric polarization of helium. The ion layer, which is almost ideally two-dimensional, lies at the liquid surface and forces responsible for its vertical equilibrium are not explicitly considered here. Furthermore, since the potential well in z for the ions is narrow and deep, and since frequencies considered here are small compared to the bounce frequency in this well, vertical motion of the ions is ignored. Finally, only modes with wave vector component $k_y = 0$ are considered. These are the Cartesian analogs of the azimuthally symmetric modes measured in the cylindrical geometry experiments of Ref. 1. The cold fluid equations which describe the two-dimensional ion system have the form

$$\frac{\partial \sigma}{\partial t} + \frac{\partial}{\partial x}(\sigma v) = 0 \quad , \tag{1}$$

$$m\left[\frac{\partial v}{\partial t} + \nu v + v\frac{\partial}{\partial x}v\right] = -q\frac{\partial}{\partial x}\left(\phi + \phi_{eo} + \phi_{ew}\right)\Big|_{z=d} \quad , \tag{2}$$

$$\nabla^2\phi = -4\pi q\sigma\delta(z-d) \quad , \tag{3}$$

where $\nabla^2 = \partial^2/\partial x^2 + \partial^2/\partial z^2$. The continuity equation (1) relates the rate of change of the areal charge density $\sigma(x,t)$ to the velocity $v(x,t)$ in the plane of the charges. Equation (2) is the equation of motion of a particle of mass m and charge q under the influence of $\phi(x,z,t)$, the potential generated by the

plasma particles, $\phi_{eo}(x,z)$, the external confinement potential and $\phi_{ew}(x,z,t)$, the external potential applied to excite waves. As indicated in the Introduction, the particle mass m is assumed to depend on the velocity as $m = m_o[1+\beta|v|^2]$. Unlike Eqs.(1) and (2) which are defined only in the plane z=d of the charges, Poisson's equation (3) is a three-dimensional equation relating the plasma potential ϕ to σ, subject to the boundary condition $\phi = 0$ on the walls $z = 0,h$ and $x = \pm L$ of the confining cell.

Before solving Eqs. (1)-(3), it is convenient to express them in terms of dimensionless variables defined as follows:

$$\frac{q}{m_o L^2 \omega_p^2}\phi \to \phi \quad , \quad \frac{q}{m_o L^2 \omega_p^2}\phi_{eo} \to \phi_{eo} \quad , \quad \frac{q}{m_o L^2 \omega_p^2}\phi_{ew} \to \phi_{ew} \quad ,$$

$$\omega_p t \to t \quad , \quad \frac{\sigma}{\sigma_o(0)} \to \sigma \quad ,$$

$$\frac{1}{L}\underset{\sim}{x} \to \underset{\sim}{x} \quad , \quad \frac{\nu}{\omega_p} \to \nu \quad ,$$

$$\frac{1}{L\omega_p} v \to v \quad , \quad (L\omega_p)^2\beta \to \beta \quad , \qquad (4)$$

where[6] $\omega_p^2 = \dfrac{4\pi q^2 \sigma_o(0)}{m_o L}$, (5)

with $\sigma_o(0)$ being the equilibrium density at x = 0. In terms of the new variables, Eqs. (1)-(3) take the form

$$\frac{\partial \sigma}{\partial t} + \frac{\partial}{\partial x}(\sigma v) = 0 \quad , \qquad (6)$$

$$[1 + \beta|v|^2]\left[\frac{\partial v}{\partial t} + \nu v + v\frac{\partial}{\partial x}v\right] = -\frac{\partial}{\partial x}(\phi + \phi_{eo} + \phi_{ew})\Big|_{z=d} \quad , \qquad (7)$$

and

$$\nabla^2\phi = -\sigma\delta(z-d) \quad . \tag{8}$$

Secular perturbation theory is used to solve Eqs. (6)-(8). The plasma variables ϕ, σ and v are expanded in a perturbation series with $\epsilon = \delta\sigma/\sigma_o$ as the small expansion parameter; σ_o is the equilibrium density and $\delta\sigma$ the density perturbation produced by a wave driven by $\phi_{ew} = \phi_{el}\cos\omega t$. The zeroth order terms of the expansion series represent the time-independent equilibrium values and the first order terms represent linear waves with a time dependence $\sim \cos\omega t$. In the absence of damping and nonlinearities, the plasma response has resonances at certain discrete values ω_{On} (n = 1, 2, . . .) of the frequency as shown in Sec. III. The inclusion of damping results in a Lorentzian resonance peak centered at ω_{On}, of width ν and amplitude ϕ_{el}/ν (for $\delta\phi$). This implies that for the perturbation expansion to be consistent, one must have $\phi_{el}/\nu\phi_o \sim O(\epsilon)$, where $\phi_o = m_o L^2\omega_p{}^2/q$. Including just the nonlinearities in Eqs. (6) and (7) gives rise, in the second order, to time-independent terms as well as second harmonic terms $\sim \cos 2\omega t$ which provide a third order correction to the equation satisfied by terms proportional to $\cos\omega t$. This has the effect of causing a shift $\sim O(\epsilon^2\omega_{On})$ in the value of the resonance frequency ω_{On}. When the damping and the nonlinearities are both effective, the resonance curve has a finite amplitude and is asymmetric about ω_{On}. To mathematically treat the two effects together, it is convenient to formally order $\nu \sim O(\epsilon^2\omega_{On})$ so that the damping and the nonlinearities first appear in the same order, namely the third; this also implies that $\phi_{el}/\phi_o \sim O(\epsilon^3)$. The resulting approximation to the solution can, however, be used for all values of ν.

With the scales $\phi_{e1} \sim 0(\varepsilon^3)$, the perturbation series for ϕ, σ and v have the form

$$\phi + \phi_{eo} + \phi_{ew} = \phi_{oo} + \phi_{eo} + [\phi_{11}e^{-i\omega t} + c.c.] + \phi_{20} + [\phi_{22}e^{-2i\omega t} + c.c.] + [(\phi_{31} + \phi_{e1})e^{-i\omega t} + c.c.] + \ldots, \quad (9)$$

$$\sigma = \sigma_{00} + [\sigma_{11}e^{-i\omega t} + c.c.] + \sigma_{20} + [\sigma_{22}e^{-2i\omega t} + c.c.] + [\sigma_{31}e^{-i\omega t} + c.c.] + \ldots, \quad (10)$$

$$v = [v_{11}e^{-i\omega t} + c.c.] + [v_{22}e^{-2i\omega t} + c.c.] + [v_{31}e^{-i\omega t} + c.c.] + \ldots, \quad (11)$$

where v_{00} and v_{20} are zero since there is no steady drift of particles in the x-direction. The components on the right-hand sides of Eqs. (9)-(11) have two subscripts, the first one referring to the order of perturbation and the second to the harmonic content. It should also be noted that the spatial dependence in Eq. (9) is on x and z while σ and v of Eqs. (10) and (11) are defined only in the plane z=d of the plasma layer.

Equations (9)-(11) are substituted in Eqs. (6)-(8) and terms with the same time dependence and the same order in ε equated. Since the modifications to the resonance curve due to nonlinearities is the primary concern of the present work, the frequency ω is written $\omega = \omega_o + \delta\omega$ where ω_o is the linear resonance frequency and $\delta\omega \equiv \omega - \omega_o \sim 0(\nu) \sim 0(\varepsilon^2\omega_o)$. The next four sections discuss the resulting equations in the first four orders of perturbation.

III. EQUILIBRIUM

In the zeroth order, the equations are time independent and describe the equilibrium density profile. In addition to the condition $v_{oo} = 0$, Eqs. (6)-(8) in the zeroth order yield

$$\frac{d}{dx}\left[\phi_{oo}(x,\ z = d) + \phi_{eo}(x, z = d)\right] = 0, \tag{12}$$

within the plasma, and

$$\left(\frac{\partial^2}{\partial x^2} + \frac{\partial^2}{\partial z^2}\right)\phi_{oo}(x,z) = -\sigma_{oo}(x)\ \delta(z-d) \quad , \tag{13}$$

subject to the boundary condition $\phi_{oo} = 0$ at the cell walls. The external potential ϕ_{eo} takes on the values ϕ_{t0}, 0 and ϕ_{b0} on the top, side and bottom of the confinement cell.

Equations (12) and (13) can be solved for the equilibrium density profile $\sigma_{oo}(x)$. Using the Green's function, Eq. (13) yields

$$\phi_{oo}(x,z = d) = \int_{-1}^{1} dx'\sigma_{oo}(x')$$

$$\times \sum_n \frac{1}{(n + \frac{1}{2})\pi} \frac{\sinh(n + \frac{1}{2})\pi d\ \sinh(n + \frac{1}{2})\pi(h-d)}{\sinh(n + \frac{1}{2})\pi h} \cos(n + \tfrac{1}{2})\pi x\ \cos(n + \tfrac{1}{2})\pi x' \ . \tag{14}$$

Substituting this result in Eq. (12) and using a discrete grid for x reduces the determination of $\sigma_{oo}(x)$ to a matrix inversion problem which can be uniquely solved for any choice of the plasma width 2a and the ratio ϕ_{t0}/ϕ_{b0}. The equilibrium profile $\sigma_{oo}(x)$, numerically obtained for the scaled values $d = 0.1$, $h = 0.2$, $a = 0.78$, $\phi_{t0}/\phi_{b0} = -7$ and for a grid with 256 points is displayed in Fig. 2. The profile is nearly rectangular with the edge becoming sharper[3] with decreasing values of h.

IV. LINEAR THEORY

Only terms oscillating at the fundamental frequency are present in the first order equations arising from Eqs. (6)-(8):

$$-i\omega_o\sigma_{11} + \frac{d}{dx}\left(\sigma_{00}\, v_{11}\right) = 0 \quad , \tag{15}$$

$$-i\omega_o v_{11} = -\frac{d}{dx}\,\phi_{11}(x, z = d) \quad , \tag{16}$$

$$\nabla^2\phi_{11} = -\sigma_{11}\,\delta(z-d) \quad . \tag{17}$$

These equations can be combined to give

$$-\omega_o{}^2\,\nabla^2\phi_{11} + \frac{\partial}{\partial x}\left[\sigma_{oo}(x)\,\frac{\partial\phi_{11}}{\partial x}\right]\delta(z-d) = 0 \quad , \tag{18}$$

which on integrating across the plasma layer $z = d$, yields

$$-\omega_o{}^2\left[\frac{\partial\phi_{11}}{\partial z}\bigg|_{d+} - \frac{\partial\phi_{11}}{\partial z}\bigg|_{d-}\right] + \frac{d}{dx}\left[\sigma_{oo}(x)\,\frac{d}{dx}\,\phi_{11}(x, z = d)\right] = 0 \ , \tag{19}$$

where ϕ_{11} satisfies the boundary condition $\phi_{11} = 0$ at the walls of the cell. Equation (19) is an eigenvalue equation which can be satisfied only for certain discrete values of ω_o. It is solved by using the expansion

$$\phi_{11}(x,z) = \sum_n B_n \frac{\cos\left(n + \frac{1}{2}\right)\pi x}{\sinh\left(n + \frac{1}{2}\right)\pi d\,\sinh\left(n + \frac{1}{2}\right)\pi(h-d)} \times$$

$$\begin{cases} \sinh\left(n + \frac{1}{2}\right)\pi d\,\sinh\left(n + \frac{1}{2}\right)\pi(h-z) \quad , & z > d \\ \sinh\left(n + \frac{1}{2}\right)\pi z\,\sinh\left(n + \frac{1}{2}\right)\pi(h-d) \quad , & z < d \end{cases} \quad , \tag{20}$$

and the orthogonality of sines and cosines to yield

$$D(\omega_o)\ B = 0 \quad , \tag{21}$$

where the elements of the matrix D are given by

$$D_{mn}(\omega_o) = \omega_o{}^2 \left(n + \tfrac{1}{2}\right) \frac{\sinh\left(n + \frac{1}{2}\right)\pi h}{\sinh\left(n + \frac{1}{2}\right)\pi d \sinh\left(n + \frac{1}{2}\right)\pi(h-d)} \delta_{mn}$$

$$- \left(n + \tfrac{1}{2}\right)\left(m + \tfrac{1}{2}\right)\pi^2 \int_{-1}^{1} dx\ \sigma_{oo}(x) \sin\left(n + \tfrac{1}{2}\right)\pi x \sin\left(m + \tfrac{1}{2}\right)\pi x \ , \tag{22}$$

and B is a vector whose components are B_n of Eq. (20). The eigenvalues ω_{01}, ω_{02}, ω_{03}, . . . for which $|D| = 0$ and the corresponding eigenfunctions ϕ_{11} are obtained numerically. As an example, the shape of $\phi_{11}(x,z = d)$ corresponding to the eigenvalue $\omega_{01} \simeq 0.83$ for the profile $\sigma_{00}(x)$ is displayed in Fig. 2. The oscillations seen in ϕ_{11} near the wall are of numerical origin. The x-dependence of the eigenfunctions on the z = d plane can be closely approximated[3] by a single cosine function inside the plasma. The approximate wave function cos 3.8x is shown as a dotted curve in Fig. 2 for comparison.

Since Eq. (18) is homogeneous, the amplitude of ϕ_{11} is undetermined within the perturbation scheme. By demanding the existence of a finite solution to the third order equation one obtains a relation (resonance curve) between the amplitude of ϕ_{11} and the frequency ω for a given external driver ϕ_{el} .

V. SECOND ORDER EQUATIONS

The second order equations contain the static (zero frequency) nonlinear distortion as well as the second harmonic response at 2ω. The zero frequency components of Eqs. (6)-(8) are

$$\frac{d}{dx}\left(\sigma_{11}v_{11}^{*} + \sigma_{11}^{*}v_{11}\right) = 0 \quad , \tag{23}$$

$$v_{11}\frac{dv_{11}^{*}}{dx} + v_{11}^{*}\frac{dv_{11}}{dx} = -\frac{d}{dx}\phi_{20}(x, z = d) \quad , \tag{24}$$

$$\nabla^2\phi_{20} = -\sigma_{20}\,\delta(z-d) \quad . \tag{25}$$

Equation (23) is trivially satisfied for σ_{11} and v_{11} given by Eqs. (15)-(17). Equation (24) relates two perfect differentials and can be integrated in x to yield the "ponderomotive" potential

$$\phi_{20}(x, z = d) = -|v_{11}|^2 + C \quad , \tag{26}$$

where C is an as yet undetermined constant. Using the Green's function technique of Sec. III, Eqs. (25) and (26) can be reduced to a matrix equation and numerically solved for σ_{20}, given v_{11} [from linear theory] and C. The value of C is chosen so that

$$\int_{-1}^{1} dx\ \sigma_{20}(x) = 0 \quad , \tag{27}$$

which implies that charge is conserved. The shape of the nonlinear static density modification, $\sigma_{20}(x)$, corresponding to the linear eigenvalue $\omega_{01} = 0.83$ is shown in Fig. 3. It is observed that the ponderomotive force enhances the plasma density at the center x=0 and at the edges $x=\pm a$ and depletes the plasma elsewhere.

The second harmonic components of Eqs. (6)-(8) are

$$- 2i\omega_o \sigma_{22} + \frac{d}{dx}\left(\sigma_{oo} v_{22} + \sigma_{11} v_{11}\right) = 0 \quad , \tag{28}$$

$$-2i\omega_o v_{22} + v_{11} \frac{dv_{11}}{dx} = - \frac{d}{dx} \phi_{22}(x, z = d) \quad , \tag{29}$$

$$\nabla^2 \phi_{22} = - \sigma_{22} \delta(x-d) \quad , \tag{30}$$

which can be combined to yield

$$- (2\omega_o)^2 \nabla^2 \phi_{22} + \frac{\partial}{\partial x}\left[\sigma_{oo}(x) \frac{\partial}{\partial x}\phi_{22}\right] \delta(z-d) =$$

$$- \frac{\partial}{\partial x}\left[\sigma_{oo}(x) v_{11} \frac{dv_{11}}{dx} + 2i\omega_o \sigma_{11} v_{11}\right] \delta(z-d) \quad . \tag{31}$$

Following Sec. IV, Eq. (31) can be expressed as a matrix equation

$$D(2\omega_o) E = F \quad , \tag{32}$$

where the matrix D is given by Eq. (22) and the vectors E and F are defined by

$$\phi_{22}(x, z = d) = \sum_n E_n \cos\left(n + \tfrac{1}{2}\right)\pi x \quad , \tag{33}$$

$$- \frac{\partial}{\partial x}\left[\sigma_{oo} v_{11} \frac{dv_{11}}{dx} + 2i\omega_o \sigma_{11} v_{11}\right] = \sum_n F_n \cos\left(n + \tfrac{1}{2}\right)\pi x \quad . \tag{34}$$

The numerical solution of Eqs. (32)-(34) for $\phi_{22}(x, z = d)$ can be readily obtained, once the first order quantities σ_{11} and v_{11} have been determined from linear theory. For the first few resonance frequencies, $2\omega_o$ is not near a zero of $|D(\omega)|$ and hence the amplitude of ϕ_{22} is small (compared to v_1^2). Thus, Eqs. (28) and (29) can be used to obtain good approximations for v_{22} and σ_{22} by ignoring ϕ_{22} in Eq. (29).

VI. THIRD ORDER EQUATIONS

The third order terms which oscillate at the fundamental frequency satisfy the equations

$$- i\delta\omega\sigma_{11} - i\omega_o\sigma_{31} + \frac{d}{dx}\left(\sigma_{oo}v_{31} + \sigma_{11}^{*}v_{22} + \sigma_{20}v_{11} + \sigma_{22}v_{11}^{*}\right) = 0 \quad , \tag{35}$$

$$- i\delta\omega v_{11} + \nu v_{11} - i\omega_o\beta|v_{11}|^2 v_{11} - i\omega_o v_{31} + v_{22}\frac{dv_{11}^{*}}{dx} + v_{11}^{*}\frac{dv_{22}}{dx} =$$

$$- \frac{d}{dx}\left[\phi_{31}(x, z = d) + \phi_{e1}(x, z = d)\right] \quad , \tag{36}$$

$$\nabla^2 \phi_{31} = - \sigma_{31}\,\delta(z-d) \quad . \tag{37}$$

These equations can be combined to yield

$$- \omega_o^2\,\nabla^2\phi_{31} + \frac{\partial}{\partial x}\left[\sigma_{oo}(x)\frac{\partial\phi_{31}}{\partial x}\right]\delta(z-d)$$

$$= \left[-2\omega_o\delta\omega\sigma_{11} - \frac{\partial}{\partial x}\left\{\sigma_o\frac{\partial}{\partial x}\left(\phi_{e1} + v_{22}v_{11}^{*}\right) + \sigma_o\nu v_{11}\right.\right.$$

$$\left.\left. + i\omega_o\left(\sigma_{11}^{*}v_{22} + \sigma_{20}v_{11} + \sigma_{22}v_{11}^{*}\right) - i\omega_o\sigma_o\beta|v_{11}|^2 v_{11}\right\}\right]\delta(z-d) \quad . \tag{38}$$

The operator acting on ϕ_{31} is the same as the linear Hermitean operator of Sec. IV. This property can be used to find a necessary condition for the existence of a bounded solution ϕ_{31} of Eq. (38). Multiplying Eq. (38) by ϕ_{11} and integrating over the volume of the cell, it is seen that the left-hand side can be integrated by parts twice using the boundary conditions $\phi_{11} = 0$, $\phi_{31} = 0$ at the walls to obtain a volume integral of ϕ_{31} multiplied by the linear operator acting on ϕ_{11}. But this is zero from Eq. (18). Therefore, the volume integral of the right-hand side of Eq. (38) multiplied by ϕ_{11} is also zero, i.e.,

$$\int_{-1}^{1} dx\ \phi_{11}(x,z=d)\ \{-2\omega_o\delta\omega\sigma_{11} - \frac{d}{dx}\left[\sigma_{oo}\frac{d}{dx}\{\phi_{e1}(x,z=d) + v_{22}v_{11}^*\}\right.$$

$$+ \sigma_o\nu v_{11} + i\omega_o(\sigma_{11}^* v_{22} + \sigma_{20}v_{11} + \sigma_{22}v_{11}^*)$$

$$\left. - i\omega_o\sigma_o\beta|v_{11}|^2 v_{11}\right]\} = 0 \quad . \tag{39}$$

Writing $\phi_{11} = A\,\hat{\phi}_{11}$ where $\hat{\phi}_{11}$ is the linear potential normalized such that Max. $\psi(x<a) = 1$ [where $\psi = \omega_0^{-1}(d/dx)\hat{\phi}_{11}(x,z=d)$] and A is the complex amplitude of ϕ_{11} in this normalization, Eq. (39) can be expressed as

$$-2\frac{\delta\omega}{\omega_o} A\,\alpha_1 + \alpha_2 - \frac{i\nu}{\omega_o} A\,\alpha_1 + |A|^2 A\,\alpha_3 = 0 \quad , \tag{40}$$

where α_1, α_2 and α_3 are real quantities defined as

$$\alpha_1 = \omega_o^2 \int_{-1}^{1} dx\ \sigma_{oo}\,\psi^2 \quad , \tag{41}$$

$$\alpha_2 = \omega_o \int_{-1}^{1} dx\ \sigma_{oo}\,\psi\frac{d}{dx}\phi_{e1}(x,z=d) \quad , \tag{42}$$

$$\alpha_3 = \int_{-1}^{1} dx\ \left\{\frac{1}{2}\sigma_{oo}\,\psi\frac{d}{dx}\left[\psi\frac{d}{dx}\left(\phi_{22} - \frac{1}{2}\psi^2\right)\right]\right.$$

$$- \frac{\psi}{2}\frac{d}{dx}(\sigma_{oo}\psi)\frac{d}{dx}\left(\phi_{22} - \frac{1}{2}\psi^2\right) + \omega_o^2\sigma_{20}\psi^2$$

$$+ \frac{1}{2}\psi^2\frac{d}{dx}\left[\frac{\sigma_{oo}}{2}\frac{d}{dx}\left(\phi_{22} - \frac{1}{2}\psi^2\right) - \psi\frac{d}{dx}(\sigma_o\psi)\right]$$

$$\left. - \omega_o^2\,\sigma_{oo}\beta\,\psi^4\right\}$$

$$\equiv \alpha_{31} + \alpha_{32} + \alpha_{33} + \alpha_{34} + \alpha_{35} \quad , \tag{43}$$

with

$$\psi = \frac{1}{\omega_o} \frac{d}{dx} \hat{\phi}_{11}(x, z = d) \quad . \tag{44}$$

As described in the previous section, ϕ_{22} can be ignored (in comparison with ψ^2) in Eq. (43) for the first few modes. Letting $A = |A|e^{i\theta}$ in Eq. (40), equating real and imaginary parts and eliminating θ yields

$$\left\{\left[2 \frac{\delta\omega}{\omega_o} \alpha_1 - \alpha_3 |A|^2\right]^2 + \frac{\nu^2 \alpha_1^2}{\omega_o^2}\right\} |A|^2 = \alpha_2^2 \quad ,$$

or

$$\left\{\left[\omega - \omega_o - \frac{\alpha_3}{2\alpha_1} \omega_o |A|^2\right]^2 + \frac{\nu^2}{4}\right\} |A|^2 = \frac{\alpha_2^2 \omega_o^2}{4\alpha_1^2} \quad . \tag{45}$$

Equation (45) gives the frequency response curve, $|A|$ vs. ω, where $|A|$ is the amplitude of ϕ_{11}, for any value of the driver ϕ_{e1} or equivalently α_2. For small values (i.e., $<<1$) of the 'nonlinearity parameter' $p \equiv (\alpha_3/2\alpha_1)(\alpha_2^2/\alpha_1^2)(\omega_o^3/\nu^3)$, $|A|$ is small and hence the term $(\alpha_3\omega_o/2\alpha_1)|A|^2$ can be ignored leading to the damped linear result, namely a Lorentzian response curve with $|A|^2 \propto [(\omega-\omega_o)^2 + \nu^2/4]^{-1}$. For $p > 1$, the effects of nonlinearity become important, causing a frequency shift $p\nu$ in the position of the response curve peak; the curve bends forwards or backwards depending on whether p (or α_3) is positive or negative. Figure 4 displays plots of normalized square amplitude $(\alpha_1^2/\alpha_2^2)(\nu^2/\omega_o^2)|A|^2$ vs. the frequency difference $(\omega-\omega_o)/\nu$ for the values 0, ±1, ±5 of p.

The numerically obtained values of α_1, α_2 and α_3 for the lowest four modes (which are of even parity in x) and for $\phi_{e1}(x = \pm L) = 1$, $\phi_{e1}(z = 0,h) = 0$ are presented in Table I. The value of β which causes the mass nonlinearity α_{35} to cancel the other nonlinearities (α_{31}, α_{32}, α_{33} and α_{34}) is denoted by β_{crit} and has the value ≈ 10 for all the modes shown. Since the

value of β [scaled as in Eq. (4)] estimated for typical experiments is $O(10^5)$, the effect of the mass nonlinearity (α_{35}) overwhelms the other nonlinearities. Since α_{35} is negative, the frequency response curve bends towards lower frequencies with increasing amplitude due to a decrease in the value of of the plasma frequency as the effective mass increases with the amplitude of the wave; this leads to a lower value of the resonance frequency.

Good approximations to the values of the coefficients α_j given in Table I can be obtained by noting that $\sigma_{oo}(x)$ [Fig. 1] can be approximated by a step-function density profile of unit height and width 2a. Also, one can write $\psi = \sin Kx$ as a consequence of the single cosine approximation to $\phi_{11}(x,z = d)$ for $|x|<a$, as illustrated in Fig. 2; the best fit values of K given in Table I can be approximated by $K_n = n\pi/a$ (corresponding to the resonance frequency ω_{on}). This leads to $\alpha_1 \simeq \omega_o{}^2 a$. Approximating $\phi_{e1}(x,z = d) \sim (4\phi_w/\pi)\exp[(x-L)/h]$ if a is not too close to L, the integral (42) can be performed yielding $\alpha_2 \simeq (-1)^{n+1}\, 8\phi_w(K_n\omega_o/h)\left[(\pi/h)^2 + K_n{}^2\right]^{-1} \exp[\pi(a-L)/h]$. Also, as mentioned in Sec. V, ϕ_{22} can be ignored in comparison with ψ^2 leading to $\alpha_{31} \simeq \alpha_{32} \simeq K_n{}^2 a/8$, $\alpha_{33} \simeq -\omega_o{}^2(K_n a/2)\sinh 2K_n h\left[\sinh 2K_n d\, \sinh 2K_n(h-d)\right]^{-1}$, $\alpha_{34} \simeq 3K_n{}^2 a/8$ and $\alpha_{35}/\beta \simeq 3\omega_o{}^2 a/4$. The estimate for α_{33} makes use of the approximation $\phi_{20}(x,z = d) = -v_1{}^2 + \text{const} \simeq -(1/2)\cos 2K_n x$ leading to

$$\phi_{20}(x,z) \simeq -\frac{\cos 2K_n x}{2\sinh 2K_n d\, \sinh 2K_n(h-d)} \begin{cases} \sinh 2K_n d\, \sinh 2K_n(h-z), & z>d \\ \sinh 2K_n z\, \sinh 2K_n(h-d), & z<d \end{cases} , \qquad (46)$$

and hence to

$$\sigma_{20}(x) = -\left[\frac{\partial\phi_{20}}{\partial z}\bigg|_{d_+} - \frac{\partial\phi_{20}}{\partial z}\bigg|_{d_-}\right] \simeq \frac{K_n \sinh 2K_n h}{\sinh 2K_n d\, \sinh 2K_n(h-d)}\cos 2K_n x \, . \qquad (47)$$

This value for σ_{20} is used in Eq. (43) along with $\psi \sim \sin K_n x$ to obtain the estimate for α_{33}.

The coefficient α_{33} represents the self-modulation effect arising from the static ponderomotive density modification σ_{20}. One can also consider the cross-modulation effect of σ_{20} (produced by the nth mode) on the frequency of the mth mode. To isolate this effect, it is convenient to use the variational principle expression[3] for ω_{om}^2 obtained by multiplying Eq. (18) by ϕ_{11} and integrating over the volume of the cell:

$$\omega_{om}^2 = \frac{\int_{-1}^{1} dx\ \sigma_{oo}(x) \left[\frac{d}{dx}\phi_{11m}(x, z = d)\right]^2}{\int_0^h dz \int_{-1}^{1} dx \left[\nabla\phi_{11m}(x,z)\right]^2} \quad . \tag{48}$$

If σ_{oo} is replaced by $\sigma_{oo} + \sigma_{20n}$ where σ_{20n} is a small static density perturbation produced by the nth mode, then the fractional change in ω_{om}^2 is

$$\frac{\delta(\omega_{om}^2)}{\omega_{om}^2} \simeq \frac{\int_{-1}^{1} dx\ \sigma_{20n}\ \psi_m^2}{\int_{-1}^{1} dx\ \sigma_{oo}\ \psi_m^2} \quad , \tag{49}$$

where $\psi_m \propto (d/dx)\phi_{11m}(x, z = d)$. Approximating σ_{oo} by a rectangular profile of width 2a and using the approximations $\psi_m \simeq \sin K_m x = \sin(m\pi x/a)$ and Eq. (47) for σ_{20n}, yields zero for the numerator on the right hand side of Eq. (49) unless m = n. Thus the ponderomotive density modification due to any mode is expected to have little effect on the resonance frequencies of other eigenmodes. In numerical computations using exact density profiles and eigenfunctions, for example, a 10% density perturbation produced by the first mode causes less than 1% change in the resonance frequencies of the next three modes.

VII. CYLINDRICAL GEOMETRY

The Cartesian results of Secs. II-VI can be extended in a straightforward manner to the azimuthally symmetric modes of relevance to the cylindrical geometry used in the experimental arrangement of Ref. 1. One again obtains Eq. (45) with $|A|$ being the amplitude of the linear mode and α_1, α_2 and α_3 given by

$$\alpha_1 = \omega_o^2 \int_{-1}^{1} r dr\, \sigma_{oo}(r)\, \psi^2 \quad , \tag{50}$$

$$\alpha_2 = \omega_o \int_{-1}^{1} r dr\, \sigma_{oo}(r)\, \psi \frac{d}{dr} \phi_{e1}(r, z = d) \quad , \tag{51}$$

$$\alpha_3 \simeq - \omega_o^2\, \beta \int_{0}^{1} r dr\, \sigma_{oo}(r)\, \psi^4 \quad , \tag{52}$$

where now the lengths (r, z, d, and h) are scaled in terms of R, the radius of the cell, the density in terms of $\sigma_{oo}(0)$, the frequencies in terms of $\omega_p \equiv [4\pi q^2 \sigma_{oo}(0)/m_o R]^{1/2}$ and β in terms of $(R\omega_p)^{-2}$. Also $\psi = \omega_o^{-1}\, (d/dr)\, \hat{\phi}_{11}(r, z = d)$. In writing Eq. (52) it is assumed that the contribution from the mass nonlinearity is the dominant effect. To find useful approximations of α_1, α_2, and α_3, it is noted that in the cylindrical case[3] also, $\sigma_{oo}(r)$ is nearly a rectangular profile of unit height and width a and $\psi \simeq J_1(j_{1n} r/a)$ to a very good approximation for $0 \leq r \leq a$. Also $\phi_{e1}(r, z = d) \simeq (4\Phi_w/\pi)\, I_o(\pi r/h)/I_o(\pi/h)$ if a is not very close to 1. In the expression for ψ and ϕ_{e1}, J and I are the Bessel function and the modified Bessel function, respectively and j_{1n} are the zeros of J_1. Using these approximations yields

$$\alpha_1 \simeq \frac{1}{2}\, \omega_o^2 a^2\, J_o^2(j_{1n}) \quad , \tag{53}$$

$$\alpha_2 \simeq \frac{-4\omega_o \Phi_w}{h} \frac{j_{1n}}{(j_{1n}/a)^2 + (\pi/h)^2} \frac{I_1(\pi a/h)}{I_o(\pi/h)} \quad J_o(j_{1n}) \quad , \tag{54}$$

and

$$\alpha_3 = - \omega_o^2 \beta \int_o^a r dr \; J_1^4\left(j_{1n} \frac{r}{a}\right) \quad . \tag{55}$$

The numerical values of α_1, α_2, α_3 [obtained from Eqs. (53)-(55)] and $p/(\beta\omega_o\Phi_w^2) = \alpha_3\alpha_2^2\omega_o^2/2\alpha_1^3\beta\Phi_w^2$ (which is independent of ω_o) are displayed in Table II for the first four azimuthally symmetric modes for typical experimental parameters[1] h = 0.2 and a = 0.895. The nonlinear frequency shift is $p\nu$ as in the Cartesian case.

VIII. CONCLUSIONS

Using a cold plasma fluid model for the ion response, a nonlinear theory of wave resonances in a two-dimensional ion layer confined under the surface of liquid helium, has been developed. Lindstedt-Poincaré theory of secular perturbation is used to calculate the nonlinear response of the plasma when damping and an external driver are both present.

It is found that the usual nonlinearities associated with the continuity equation and the equation of motion give rise to a positive nonlinear shift in the value of the resonance frequency. However, the experimentally measured frequency shifts are negative.

A survey of the experiments suggests the possibility of another source of nonlinearity, namely, a quadratic dependence of the effective mass of a plasma particle on its velocity. For instance, it has been observed[1] that the effective mass of an ion increases roughly linearly with the temperature of liquid helium, from a value ~35.2 m_{He} at 0.1K to ~39.6 m_{He} at 0.4 K for an ion density of 7×10^7 cm^{-2}. Postulating that the oscillatory motion of an ion due to a wave corresponds to an increased effective temperature with $\Delta T = m|v|^2$ (for one-dimensional motion), one obtains $m = m_o[1 + \beta|v|^2]$ where $m_o \simeq 34\ m_{He}$ and $\beta = 6.7\times10^{-7}\ cm^{-2}s^2$. Scaled in terms of $(R\omega_p)^{-2}$ where R is the cell radius and $\omega_p = [4\pi q^2\sigma_o(0)/mR]^{1/2}$, the coefficient β has the estimated value $\simeq 9\times10^5$. The increase in the mass with the amplitude of the wave leads to a decrease in the value of ω_p and to a decrease in the value of the resonance frequencies. The large value of the scaled β insures that the negative shift of the resonance frequency due to mass nonlinearity overwhelms the contributions from the nonlinear terms in the continuity equation and the equation of motion. Using Table II and the value[1] $\nu = 2.74\times10^{-2}\ \omega_p$, one obtains, for the lowest azimuthally symmetric mode, $\omega_{NL}^2 = \omega_L^2\ (1 - \zeta\ \Phi_w^2)$

where Φ_w is measured in volts and $\zeta \simeq 1100\ V^{-2}$. This value of ζ is to be compared against the experimental value of $200\ V^{-2}$. There is also some experimental evidence[7] that ν also increases nonlinearly with amplitude; this would lower the theoretical prediction for ζ. However, the important point is that our conjecture of a mass nonlinearity gives the correct sign of the effect and yields results close to the experimentally observed values, in spite of various uncertainties regarding indirect measurements.

Since at the present time there does not exist a first-principles theory capable of predicting the value of β, and since it is also possible that its value may vary from one experimental set-up to another, in this study we have introduced the concept of a critical β. Its numerical value is illustrated in Table I. Physically, β_{crit} defines the regime beyond which the usual fluid nonlinearities become less important than the mass nonlinearity. This may be a useful tool in assessing the operational regime of future experiments.

ACKNOWLEDGEMENTS

We wish to thank Prof. G. Williams, S. Hannahs and A. Greenfield for useful discussions about their experiments which motivated this work.

This work is sponsored by the Office of Naval Research.

REFERENCES

1. M.L. Ott-Rowland, V. Kotsubo, J. Theobald and G. Williams, Phys. Rev. Lett. 49, 1708 (1982).

2. C.F. Barenghi, C.J. Mellor, C.M. Muirhead and W.F. Vinen, J. Phys. C 19, 1135 (1986).

3. S.A. Prasad and G.J. Morales, Phys. Fluids (to be published).

4. L.D. Landau and E.M. Lifshitz, Fluid Mechanics (Pergamon, Oxford, 1959), ch. 1, sec. 11.

5. H. Ikezi, Phys. Rev. B27, 585 (1983).

6. Note the difference in the definition of ω_p^2 in Ref. 3 where $\omega_p^2 = 4\pi q^2 \sigma_o(0)/m_o h$.

7. G. Williams (private communication).

FIGURE CAPTIONS

Fig. 1 Cartesian model geometry.

Fig. 2 Scaled equilibrium density profile $\sigma_{oo}(x)$ for the scaled (to L) values d = 0.1, h = 0.2, a = 0.78, $\phi_{to}/\phi_{bo} = -7$ and the eigenfunction $\phi_{11}(x,z = d)$ (solid curve) corresponding to the lowest eigenvalue $\omega_{01} \simeq 0.83$. The dots are a plot of cos3.8x.

Fig. 3 Nonlinear static density modification $\sigma_{20}(x)$ (produced by ϕ_{11} of Fig. 2) scaled in terms of 100 [Max $v_{11}(x < a)$]^2.

Fig. 4 Frequency response curve in which the square of the amplitude |A| is plotted vs. the driver frequency for the values 0, ±1, ±5 of the 'nonlinear' parameter $p = (\alpha_3/2\alpha_1)(\alpha_2^2/\alpha_1^2)(\omega_o^3/\nu^3)$.

TABLE CAPTIONS

TABLE I. Scaled numerical values of ω_o, K, α_1, α_2, α_{31}, α_{32}, α_{33}, α_{34} and α_{35}/β for Cartesian geometry and the scaled (to L) values d = 0.1, h = 0.2, a = 0.78 and $\phi_{to}/\phi_{bo} = -7$. β_{crit} is the value of β for which the frequency shift produced by the mass nonlinearity cancels the frequency shift produced by fluid nonlinearities.

TABLE II. Scaled numerical values of α_1, α_2, α_3 and the nonlinearity parameter p obtained from the approximate Eqs. (53)-(55) for the scaled (to L) values d = 0.1, h = 0.2, a = 0.895 corresponding to typical experiments in cylindrical geometry.

TABLE I.

n	ω_{on}	K_n	α_1	α_2	α_{31}	α_{32}	α_{33}	α_{34}	α_{35}/β	$\beta_{crit} = -\beta \sum_{i=1}^{4} \alpha_{3i}/\alpha_{35}$
1	0.83	3.8	0.56	-0.0022	1.54	1.54	- 3.25	4.56	-0.42	10.45
2	1.56	7.6	1.97	0.0068	6.39	6.39	-15.82	18.45	-1.49	10.34
3	2.15	11.4	3.68	-0.103	14.36	14.36	-41.15	41.10	-2.80	10.24
4	2.62	15.2	5.40	0.114	24.85	24.85	-80.00	71.25	-4.09	10.01

TABLE II.

n	ω_o	α_1/ω_o^2	$\alpha_2/(\omega_o \Phi_w)$	$\alpha_3/(\omega_o^2 \beta)$	$p/(\beta\omega_o \Phi w^2) = \alpha_3\alpha_2^2\omega_o^2/(2\alpha_1^3\ \beta\Phi_w^2)$
1	0.87	0.065	0.024	0.016	0.017
2	1.53	0.036	-0.028	0.006	0.052
3	2.07	0.025	0.027	0.003	0.084
4	2.51	0.019	-0.025	0.002	0.101

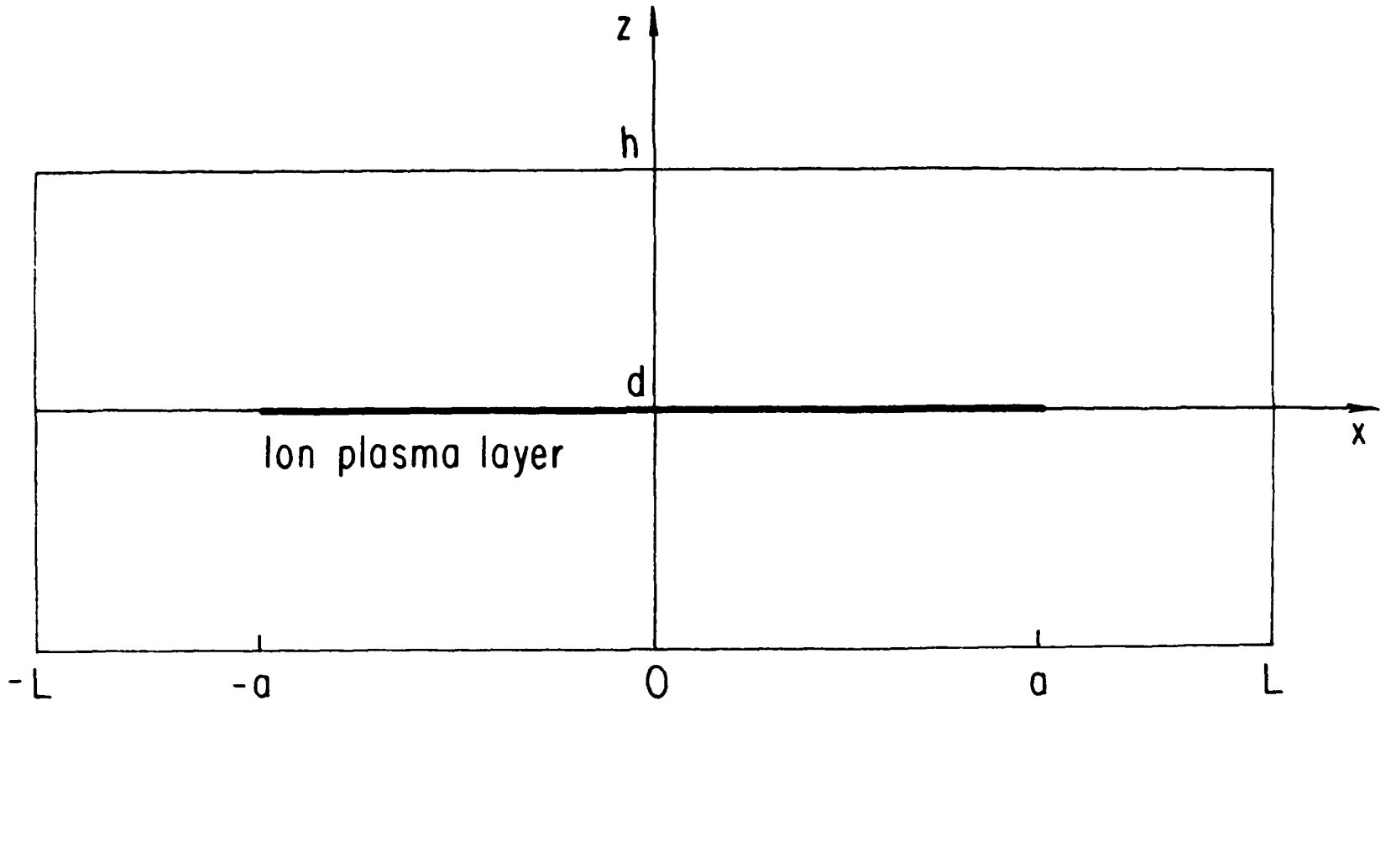

Fig. 1

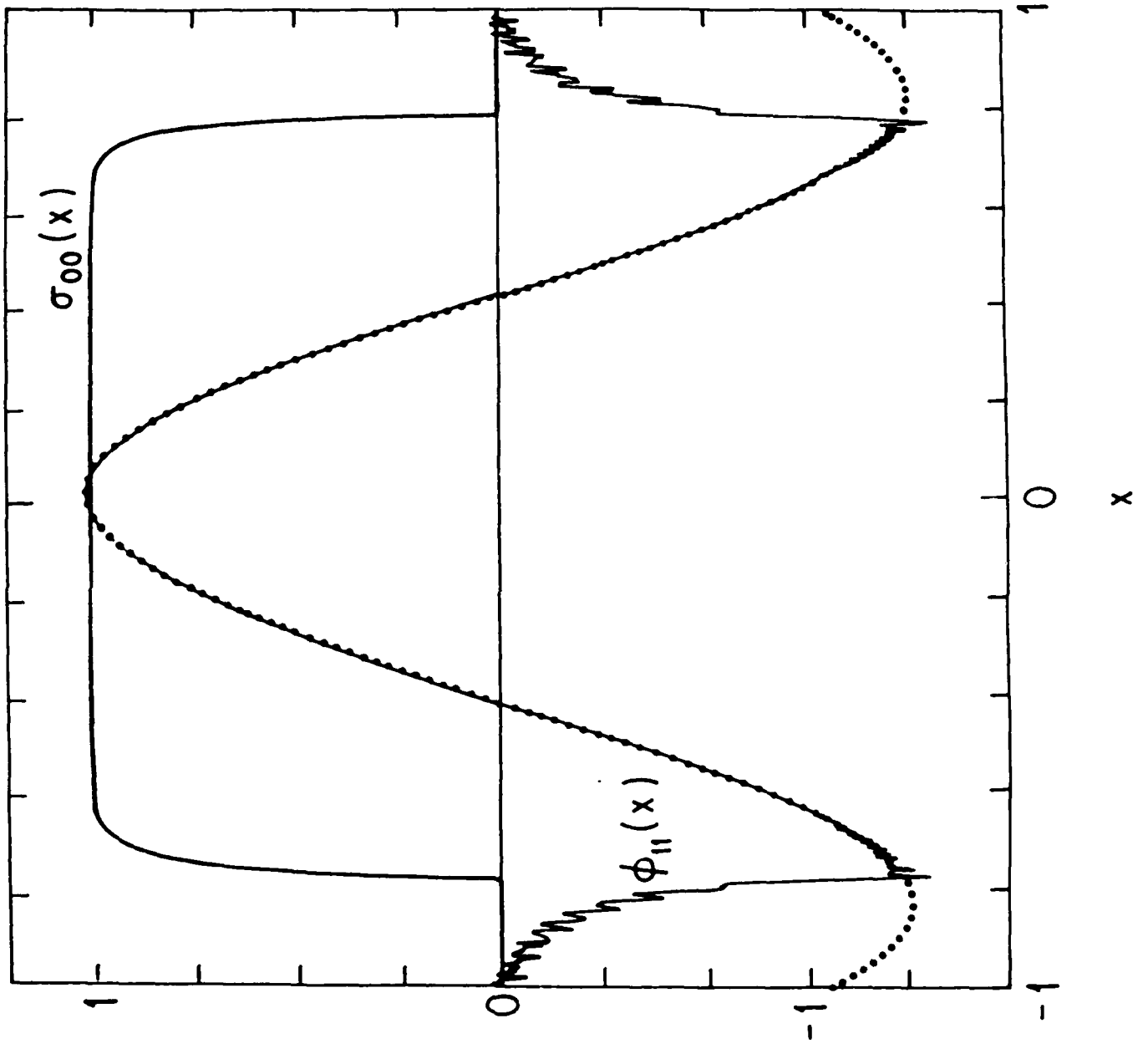

Fig. 2

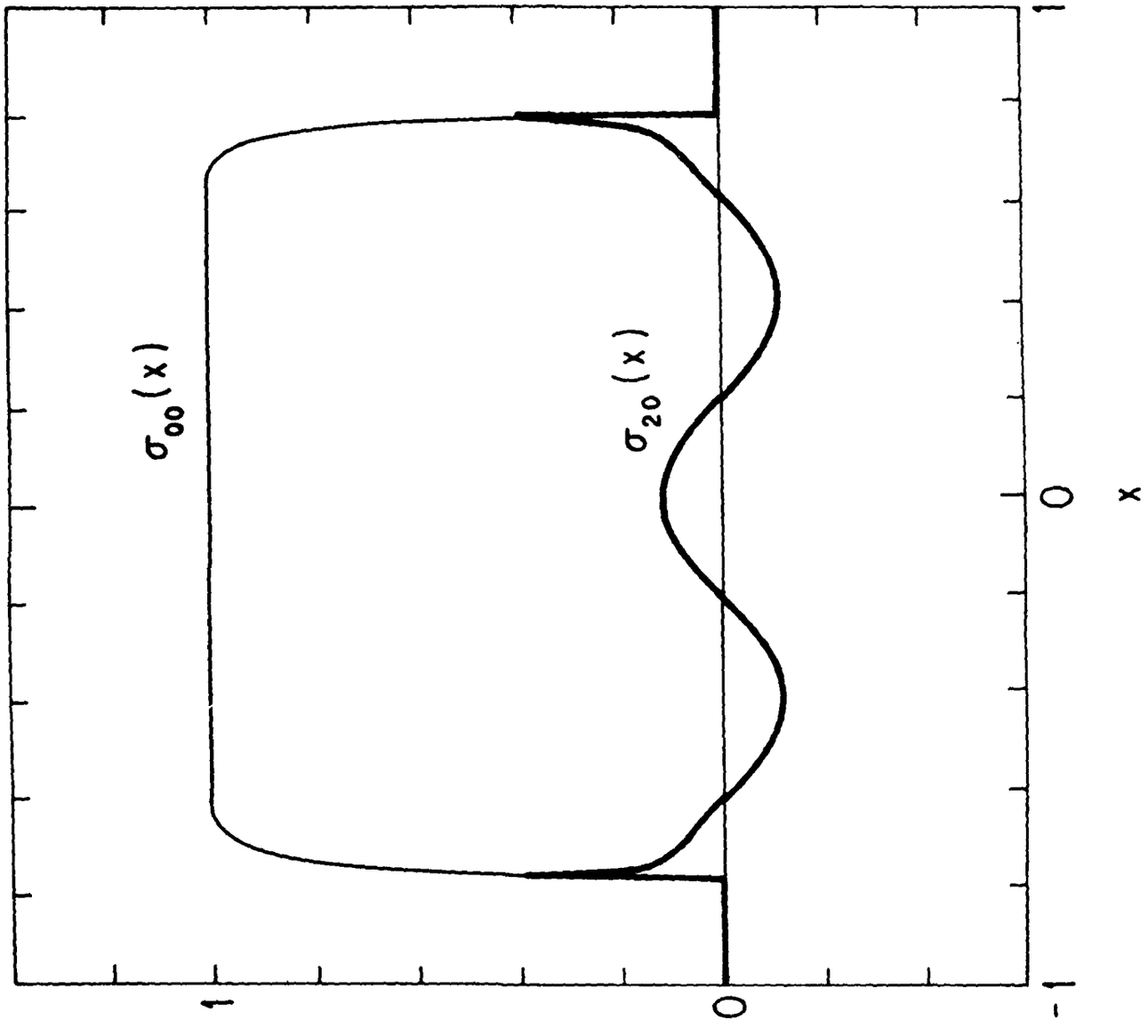

Fig. 3

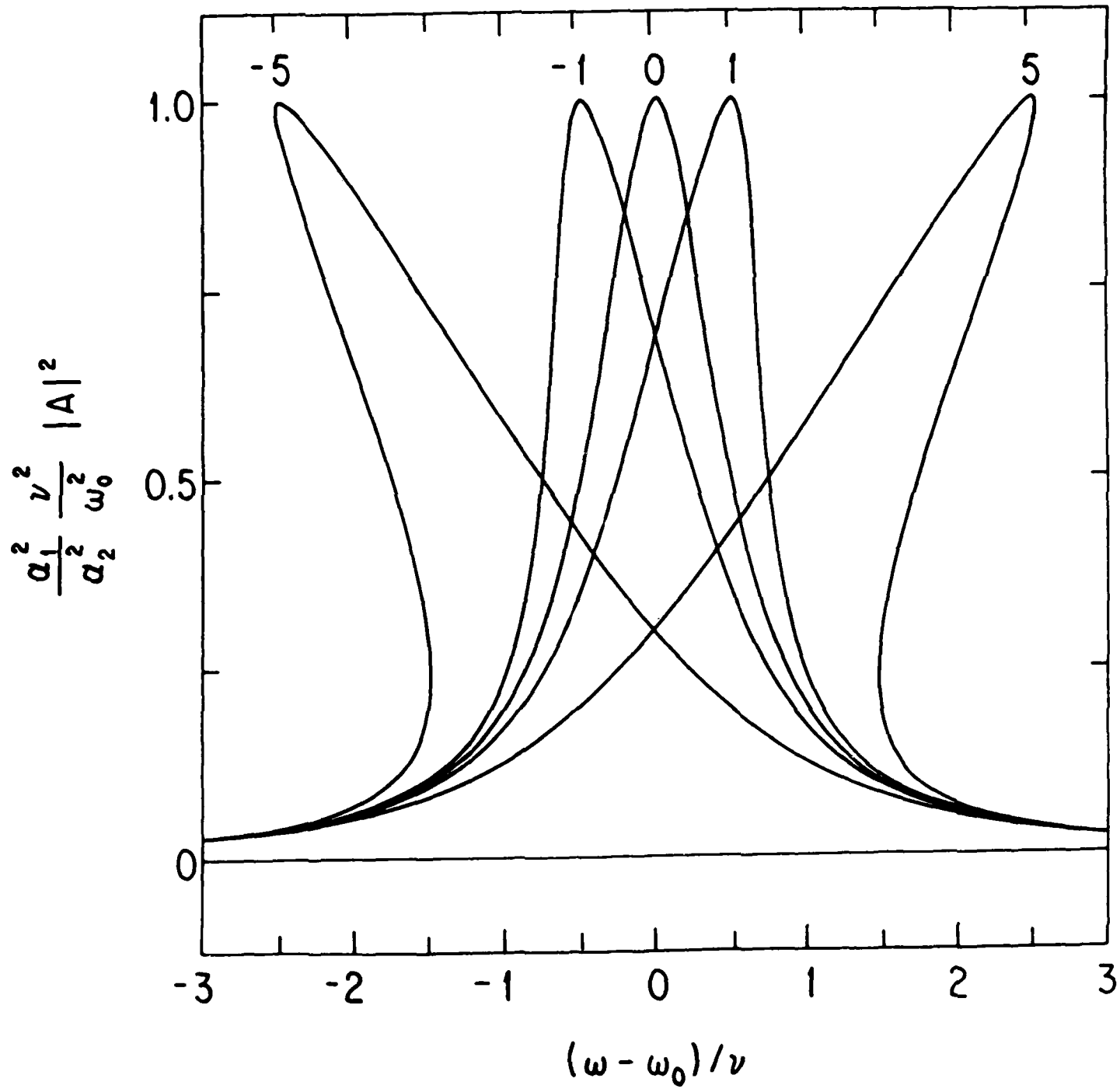
-5
-1
0
1
5
1.0
0.5
0
-3
-2
-1
0
1
2
3
$\frac{a_1^2}{a_2^2}\frac{\nu^2}{\omega_0^2}|A|^2$
$(\omega-\omega_0)/\nu$

Fig. 4

PPG-1092 "Measurement of Parallel Ion Energy Distribution Function in PISCES Plasma," G.R. Tynan, D.N. Goebel, B. LaBombard, Y. Hirooka, W.K. Leung, and R.W. Conn, August 1987.

PPG-1093 "Stochastic Theory of Diffusional Planar Atomic Clustering", N.M. Ghoniem, August 1987 (total revision of PPG-987).

PPG-1094 "Particle Simulation of a High Power Gyrotron Oscillator", A.T. Lin, Z.H. Yang, and K.R. Chu, August 1987.

PPG-1095 "Computer Simulation of Dislocation Pattern Formation," N. M. Ghoniem, R. Amodeo, August 1987.

PPG-1096 "Determination of the Bias Factor by the Moments Solution to the Fokker-Planck Equation," N.M. Ghoniem, to be submitted to Journal of Nuclear Materials, August, 1987.

PPG-1097 "Binary Collision Monte Carlo Simulations of Cascades in Polyatomic Ceramics," N. M. Ghoniem, S. P. Chou, to be submitted to Journal of Nuclear Materials, August 1987.

PPG-1098 "A Three Dimensional MHD Simulation of the Interaction of the Solar Wind with Comet Halley", P. Ogino, R.J. Walker, and M. Ashour-Abdalla, JGR, August 1987.

PPG-1099 "Observation of Large Scale Modification in the Polar Ionosphere by High Power Electromagnetic Waves", A.Y. Wong, P.Y. Cheung, M. McCarrick, J. Stanley, R. Wuerker, and E. Fremouw, September 1987.

PPG-1100 "Titan Reverse Field Pinch Fusion Reactor Study: Interim Report," F. Najmadbadi, N. Ghoniem, R. W. Conn, March, 1987.

PPG-1101 "Experimental Measurement of Electron Particle Diffusion from Sawtooth Induced Density Pulse Propagation in TEXT", S. K. Kim and D. L. Brower, W. A. Peebles, and N. C. Luhmann, Jr., submitted to Phys. Rev. Lett., September 1987.

PPG-1102 "San Diego Abstracts--Papers for the San Diego Meeting of the Division of Plasma Physics, American Physical Society, November 2-6, 1987, Carole Conn, ed., September 1987.

PPG-1103 "Instability of the Sheath Plasma Resonance", R. Stenzel, Phys. Rev. Lett., September 1987.

PPG-1104 "Simulation of Transient Behavior in a Pulse-Line Driven Gyrotron Oscillator", A.T. Lin, Chih-Chien Lin, Z.H. Yang, K.R. Chu, A.W. Fliflet, and S. Gold, submitted to IEEE Trans.-PS special issue, September 1987.

PPG-1105 "Intrinsic Electron Transport Caused by Absorption of a Fast Alfven Wave", D. Jovanovic and G.J. Morales, submitted to The Physics of Fluids, September, 1987.

PPG-1106 "Nonlinear Resonance of Two-Dimensional Ion Layers", S.A. Prasad and G.J. Morales, submitted to The Physics of Fluids, September, 1987.

END

3-88

DTIC